IVYSPRING INTERNATIONAL PUBLISHER

Theranostics

2017; 7(11): 2863-2877. doi: 10.7150/thno.19353

Research Paper

Silencing Of Circular RNA-ZNF609 Ameliorates Vascular Endothelial Dysfunction

Chang Liu[1, 2*], Mu-Di Yao[2, 3*], Chao-Peng Li[4*], Kun Shan[1*], Hong Yang[2, 3], Jia-Jian Wang[1], Ban Liu[5], Xiu-Miao Li[3], Jin Yao[2, 3], Qin Jiang[2, 3✉], Biao Yan[1, 6, 7✉]

1. Eye Institute, Eye & ENT Hospital, Shanghai Medical College, Fudan University, Shanghai, China;
2. The Fourth School of Clinical Medicine, Nanjing Medical University, Nanjing, China;
3. Eye Hospital, Nanjing Medical University, Nanjing, China;
4. Department of Ophthalmology, Huai'an First People's Hospital, Nanjing Medical University, Jiangsu, China;
5. Department of Cardiology, Shanghai Tenth People's Hospital, Tongji University School of Medicine, Shanghai, China;
6. Shanghai Key Laboratory of Visual Impairment and Restoration, Shanghai, China;
7. State Key Laboratory of Molecular Engineering of Polymers (Fudan University), Shanghai, China.

* These authors contributed equally to this work.

✉ Corresponding authors: Biao Yan E-mail: biao.yan@fdeent.org Tel: 86-21-64377134 Fax: 86-21-64377134 Fudan University, 83 Fen Yang Road, Shanghai, China 200030 Or Qin Jiang E-mail: jqin710@vip.sina.com Tel: 86-25-86677677 Fax: 86-25-86677677 Eye Hospital, 138 Han Zhong Road, Nanjing, China 210000

Received: 2017.01.25; Accepted: 2017.05.08; Published: 2017.07.08

Abstract

Vascular dysfunction is a hallmark of ischemic, cancer, and inflammatory diseases, contributing to disease progression. Circular RNAs (circRNAs) are endogenous non-coding RNAs, which have been reported to be abnormally expressed in many human diseases. In this study, we used retinal vasculature to determine the role of circular RNA in vascular dysfunction. We revealed that cZNF609 was significantly up-regulated upon high glucose and hypoxia stress *in vivo* and *in vitro*. cZNF609 silencing decreased retinal vessel loss and suppressed pathological angiogenesis *in vivo*. cZNF609 silencing increased endothelial cell migration and tube formation, and protected endothelial cell against oxidative stress and hypoxia stress *in vitro*. By contrast, transgenic overexpression of cZNF609 showed an opposite effects. cZNF609 acted as an endogenous miR-615-5p sponge to sequester and inhibit miR-615-5p activity, which led to increased MEF2A expression. MEF2A overexpression could rescue cZNF609 silencing-mediated effects on endothelial cell migration, tube formation, and apoptosis. Moreover, dysregulated cZNF609 expression was detected in the clinical samples of the patients with diabetes, hypertension, and coronary artery disease. Intervention of cZNF609 expression is promising therapy for vascular dysfunction.

Key words: vascular dysfunction, circular RNAs, microRNA sponge, retinopathy of prematurity, diabetic retinopathy.

Introduction

Vascular dysfunction occurs in many malignant, inflammatory, ischemic, infectious and immune disorders [1, 2]. These disorders are usually accompanied by endothelial barrier breakdown, vascular leakage, inflammatory response, and angiogenesis [3]. Endothelial cells are involved in the regulation of vascular function homeostasis. Endothelial dysfunction is implicated in several pathological processes [4, 5]. Thus, targeting vascular endothelial dysfunction has enormous therapeutic interest in the prevention and treatment of vascular complications.

Circular RNAs (circRNAs) are a novel class of non-coding RNAs that form a covalently closed continuous loop [6, 7]. The majorities of circRNAs are highly conserved across species, and often show tissue- or development-specific expression pattern [8]. Aberrant circRNA expressions have been detected in

several cardiovascular diseases and cancers, which are usually accompanied by vascular dysfunction [9-11]. Vascular dysfunction is often associated with abnormal gene regulation and endothelial cell dysfunction [12, 13]. circRNAs can regulate gene expression by functioning as microRNA (miRNA) sponges or regulators of gene splicing and transcription. They are also potential regulators of cell function [14]. Inspired by these findings, we speculate that circRNAs are potentially involved in vascular dysfunction.

Retinal vasculature can be viewed directly and noninvasively, providing a window to investigate the mechanism of vascular dysfunction [15]. Ischemic retinopathies, such as retinopathy of prematurity (ROP) and diabetic retinopathy (DR), share several common pathological features, including vessel loss and consequent pathological angiogenesis. In this study, we employed retinal vasculature to investigate the role of circular RNA in vascular dysfunction. cZNF609 was identified as one of the Top 10 abundantly expressed circular RNAs in endothelial cells [6]. circBase retrieval shows that one isoform of cZNF609 is highly conserved between mouse and human genome, which is located at chr15:64791491-64792365 in human genome and chr9:65642428-65643302 in mouse genome (Figure S1) [16, 17]. The host gene, ZNF609, is a member of Zinc finger protein family. Zinc finger proteins play important roles in DNA recognition, RNA packaging, transcriptional activation, regulation of apoptosis, protein folding and assembly, and lipid binding [18]. We speculate that circular RNA generating from ZNF609 may also regulate these processes. Abnormal transcriptional activation, apoptosis, and protein function is implicated in retinal vascular dysfunction. Based on above-mentioned evidences, we speculate that circular RNA generating from ZNF609 would potentially regulate retinal vascular dysfunction.

In this study, we characterized the expression pattern of circular RNA-ZNF609 and investigated its role in retinal vascular dysfunction. We revealed that silencing cZNF609 could protect endothelial cells against hypoxic and oxidative stress *in vitro*, decrease retinal vessel loss and suppress pathological angiogenesis *in vivo*. Intervention of circular RNA expression would provide a novel insight into the therapeutics of vascular diseases.

Materials and Methods

Ethics statement

Animal experiments were approved by the Animal Care and Use Committee of Eye & ENT Hospital and Nanjing Medical University. The animals were bred and housed in the pathogen-free animal facility and fed a standard normal diet ad libitum with free access to water. They were also handled in agreement with the guidelines of the Statement for the Use of Animals in Ophthalmic and Vision Research (ARVO). The surgical specimens were handled according to the Declaration of Helsinki. All patients gave the informed consent before inclusion.

Cell culture and transfection

HUVECs were cultured in Dulbecco's Modified Eagle Medium/F12 (GIBCO) containing 10% fetal bovine serum (FBS) plus endothelial cell growth supplement (ECGS) (BD Biosciences, Bedford, MA) at 37°C in 5% CO_2 and 95% humidity. HUVECs were transfected with small interfering RNAs (siRNAs; Sigma, St Louis, MO) targeting cZNF609 using Lipofectamine RNAiMax (Life Technologies, Carlsbad, CA) according to the manufacturer's protocol.

Oxygen-induced retinopathy (OIR) model

The OIR mouse model was generated using C57BL/6 mice [19]. Briefly, the newborn mice at P7 and their nursing mothers were exposed to 75% oxygen in a hyperoxic chamber for 5 days, and then returned to room air for 5 days. Age-matched mice in room air were taken as the normoxic control group.

Induction of diabetes mellitus

Diabetes mellitus was induced in 8-week-old male C57BL/6 mice by intraperitoneal injection of streptozotocin (150 mg/kg, STZ, Sigma Aldrich) dissolved in citrate buffer. Control animals received an injection of equal volume of citrate buffer. Blood glucose levels were detected every week after STZ administration. Induction of diabetes mellitus was defined in mice when the non-fasting blood glucose levels were >250 mg/dL.

Assessment of acellular capillaries

Retinal vasculature was isolated by trypsin digestion method. Briefly, freshly isolated eyes were fixed with 10% buffered formalin overnight. The retinas were carefully removed, and digested in 2% trypsin solution for 3 h at 37°C. Retinas were washed for 5 min. Retinal vasculature was dried for 30 min at 37°C and stained with periodic acid Schiff and hematoxylin.

Vascular permeability assay

C57BL/6 mice were anesthetized with ketamine and xylazine. Evans blue (30 mg/kg) was injected into the vein, and followed by injection of bradykinin. One hour after Evans blue injection, the chest was opened.

An 18-gauge cannula was inserted through the ventricle into the ascending aorta. The intravascular dye was flushed. The cornea, lens and vitreous humour were removed, and retinas and sclera were fixed in 4% paraformaldehyde in PBS for 30 min at room temperature. The retinas were treated with dimethylformamide (Sigma Aldrich, St. Louis, MO) overnight at 78 °C, and then centrifuged at 12,000 g for 15 min. The supernatant was detected spectrophotometrically at 620 nm (blue) and 740 nm (background).

Preparation of nuclear and cytoplasmic fraction

The nuclear and cytoplasmic fractions were extracted using NE-PER Nuclear and Cytoplasmic Extraction Reagents (Thermo Scientific) according to the manufacturer's instructions. Briefly, HUVECs were cultured in 150-mm dishes for 48 h to achieve about 80% confluence. About 2 × 10^6 cells were harvested, washed with cold 1× PBS twice followed by centrifugation at 500 × *g* for 5 min. The pellet was resuspended and incubated with Cytoplasmic Extraction Reagent I. Cell membrane was disrupted by vigorous vortexing for 15 s and incubation on ice for 10 min. Next, the Cytoplasmic Extraction Reagent II was added followed by vortexing for 5 s and incubation for 3 min. The nuclear and cytoplasmic portions were separated by centrifuging at 1,500 × *g* for 5 min.

RNase R treatment

For RNase R treatment, about 2 μg of total RNAs were incubated with or without 3U μg $^{-1}$ of RNase R for 30 min at 37° C. The resulting RNAs were subsequently purified using an RNeasy MinElute cleaning Kit (Qiagen).

Statistical analysis

All data were expressed as means ±SEM. Statistical analysis was performed using Student's *t* test or analysis of variance (ANOVA) followed by Fisher's least-significant-difference post hoc test for multiple comparison. $^*P < 0.05$ was considered statistically significant.

Results

Expression pattern of cZNF609 upon vascular dysfunction *in vivo* and *in vitro*

Quantitative reverse transcriptase-PCR (qRT-PCR) assays showed that cZNF609 was expressed in several endothelial cells derived from different human vascular beds (Figure 1A). The amplified product of cZNF609 was sent for sequencing. The sequencing result was completely in accordance with cZNF609 sequence in circBase (Figure 1B). qRT-PCRs and fluorescence *in situ* hybridization (FISH) assays revealed that cZNF609 was mainly expressed in the cytoplasm of HUVECs (Figure 1C and 1D). We then detected cZNF609 stability after actinomycin D (an inhibitor of transcription) treatment. cZNF609 was highly stable with a half-life >24 h, whereas ZNF609 mRNA was easily degraded with a half-life of <6 h (Figure 1E). cZNF609 was resistant to RNase R digestion, whereas linear ZNF609 mRNA and VEGFA mRNA was easily degraded (Figure 1F).

We then determined whether cZNF609 expression is altered upon stress *in vitro*. HUVECs were exposed to high glucose medium to mimic diabetic condition. High glucose increased cZNF609 expression in a time-dependant manner (Figure 1G). cZNF609 expression in diabetic retinas was significantly higher than that in non-diabetic controls (Figure 1H). In the mouse model of oxygen-induced retinopathy (OIR), retinal cZNF609 expression was significantly down-regulated at the vaso-obliteration stage (P7-P12), whereas up-regulated at the neovascularization stage (P12-P17) (Figure 1I). We also showed high glucose treatment did not alter ZNF609 mRNA expression. Retinal ZNF609 mRNA expression was not altered in the retinas of diabetic mice and OIR mice (Figure S2A-C).

cZNF609 silencing decreases retinal vessel loss and suppresses pathological angiogenesis *in vivo*

Ischemic retinopathies such as retinopathy of prematurity and diabetic retinopathy have two common pathological features, including vessel loss and consequent pathologic angiogenesis [20]. We then employed the two animal models to investigate the effect of cZNF609 silencing on vascular dysfunction.

We designed 3 different shRNAs for cZNF609 silencing, including a shRNA targeting the backsplice sequence of cZNF609 (shRNA1), a shRNA targeting the sequence only existed in ZNF609 linear transcript (shRNA2), and a shRNA targeting the sequence shared by both linear and circular ZNF609 transcript (shRNA3). shRNA1 or shRNA3 transfection significantly down-regulated cZNF609 expression. shRNA1 had greater silencing efficiency than shRNA3 (Figure S3A). We selected shRNA1 for cZNF609 silencing due to its silencing efficiency and specificity. cZNF609 shRNA1 injection significantly reduced retinal cZNF609 expression throughout the experiment (Figure S3B).

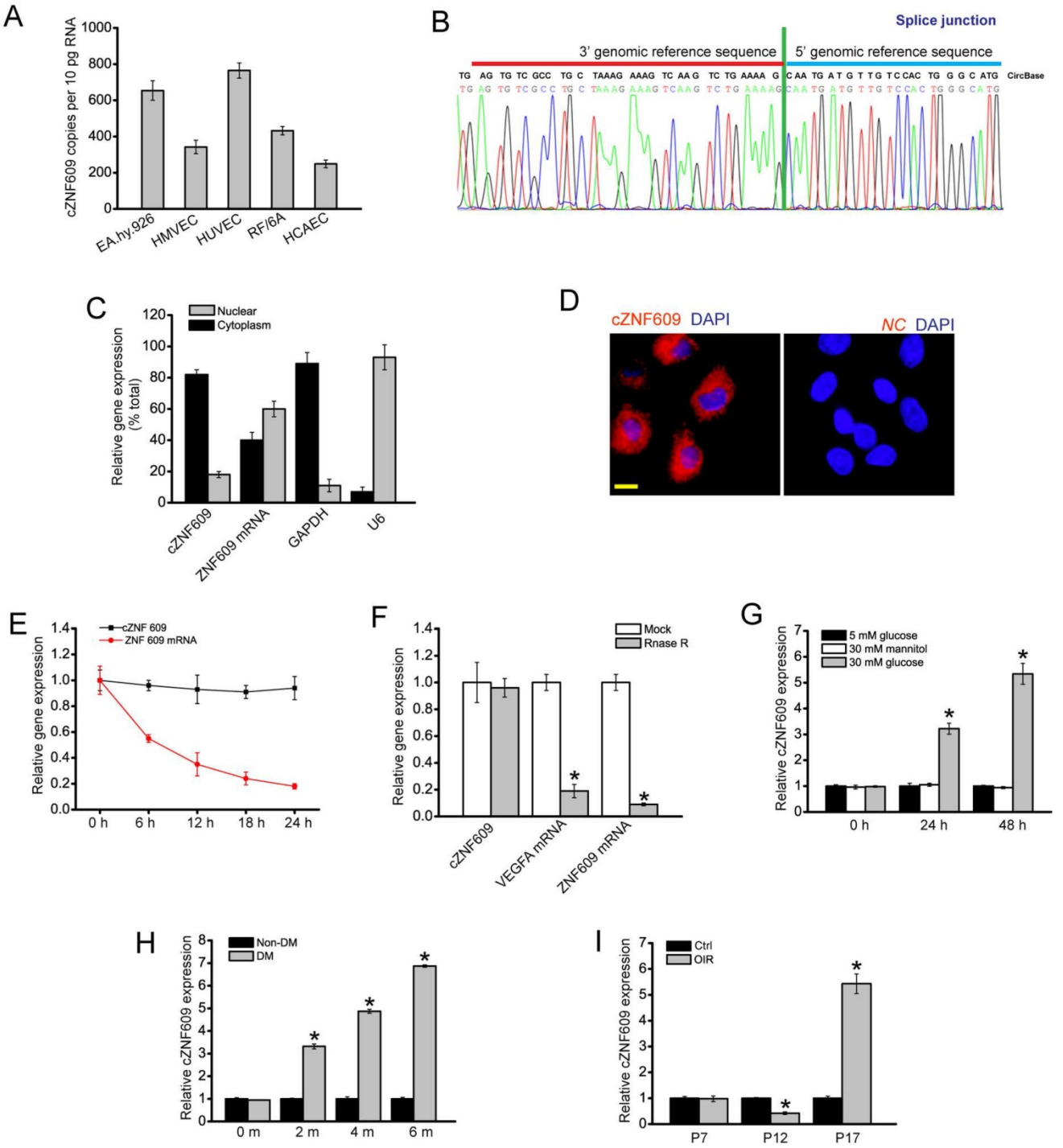

Figure 1. Expression pattern of cZNF609 during vascular dysfunction *in vivo* and *in vitro* (A) Absolute quantification for cZNF609 expression in endothelial cells from different sources, including EA.hy.926 cells, HMVECs, HUVECs, RF/6A cells, and HCAECs (n=4). (B) The sequence of cZNF609 was obtained from Sanger sequencing. (C) The expression levels of nuclear control transcript (U6), cytoplasmic control transcript (GAPDH), ZNF609 mRNA, and cZNF609 were determined by qRT-PCRs in the nuclear and cytoplasmic fractions of HUVECs (n=4). (D) RNA-FISH assays were conducted to detect cZNF609 expression distribution in HUVECs using Cy3-labeled sense (negative control, *NC*) and antisense probes (cZNF609). Nuclei were stained with 4, 6-diamidino-2-phenylindole (DAPI). Blue, DAPI; cZNF609, red. Scale bar, 20 μm. (E) qRT-PCRs were conducted to detect the amount of cZNF609 and ZNF609 mRNA after actinomycin D treatment for the indicated time points in HUVECs (n=4). (F) Total RNAs were digested with RNase R followed by qRT-PCRs detection of cZNF609 expression. Vascular endothelial growth factor A (VEGFA) and ZNF609 mRNA was detected as the RNase R-sensitive controls (n=4, **P*<0.05 versus Mock). (G) HUVECs were incubated with the medium containing 5 mM glucose, 30 mM glucose, or 30 mM mannitol for the indicated time points. The group treated with mannitol was taken as the osmolar control. qRT-PCRs were conducted to detect cZNF609 expression (n=4, **P*<0.05 versus 5 mM glucose). (H) qRT-PCRs were conducted to detect cZNF609 expression in the retinas of C57BL/6 mice after 2, 4, and 6-month diabetes mellitus induction (n=6 animals per group, **P*<0.05 versus non-DM). (I) Neonatal C57BL/6 mice were exposed to 75% oxygen from P7 to P12, and then returned to room air. qRT-PCRs were conducted to compare cZNF609 expression between un-treated (Ctrl) and OIR retinas at the indicated time points (n=6 animals per group, **P*<0.05 versus Ctrl). All data were from at least three independent experiments.

We first determined whether cZNF609 silencing affected normal retinal vasculature development. We did not observe significant difference of vascularized area, tip cell numbers, and branching points between cZNF609 silencing group and control group at P5 and P7 (Figure S4 A-C). At P17, cZNF609 silencing did not affect pericyte coverage (Figure S4D). The ganglion cell layer (GCL), inner nuclear layer (INL), and outer nuclear layer (ONL) was histologically similar between cZNF609 silencing and control group (Figure S4E). Thus, cZNF609 silencing did not affect normal retinal vasculature development.

In the model of diabetic retinopathy, retinal trypsin digestion assays showed that cZNF609 silencing rescued hyperglycemia-induced aggravated capillary degeneration (Figure 2A). Evans blue assays showed that cZNF609 silencing decreased diabetes mellitus-induced retinal vascular leakage (Figure 2B). ELISA assays showed that cZNF609 silencing decreased retinal inflammation response, as shown by lower retinal expression of C-reactive protein (CRP), MCP-1, VEGF, interleukin (IL)-1, IL-6, and TNF-α (Figure 2C).

In the mouse model of oxygen-induced retinopathy, there was a dramatic reduction in avascular area in cZNF609 silencing retinas compared with age-matched controls at postnatal day 12 (P12) and P17. cZNF609 silencing mice also decreased pathological retinal angiogenesis (2-fold decrease) (Figure 2D).

cZNF609 regulates endothelial cell function *in vitro*

Endothelial dysfunction is a major mediator of vascular dysfunction [21]. We thus investigated the role of cZNF609 in endothelial cell *in vitro*. We designed three different small interfering RNAs (siRNAs) for cZNF609 silencing. siRNA1 or siRNA3 transfection significantly down-regulated cZNF609 expression (Figure 3A).

We first determined the effect of cZNF609 silencing on endothelial cell function under basal condition and stress condition. cZNF609 silencing by siRNA1 or siRNA3 led to increased cell viability (Figure 3B), increased proliferation (Figure 3C), and accelerated cell migration and tube formation (Figure 3D, 3E, and S5). Oxidative stress and hypoxic stress are tightly associated with vascular dysfunction [22]. PI staining and caspase 3 activity assays revealed that cZNF609 silencing by siRNA1 or siRNA3 partially rescued HUVECs from oxidative or hypoxic stress-induced cell apoptosis as shown by less PI-positive cells (dying or dead cells) and decreased caspase 3 activity (Figure S6, S7, and S8).

We further conducted the gain of function analysis of cZNF609, and detected whether cZNF609 is sufficient alone to drive endothelial phenotypes. We revealed that cZNF609 overexpression significantly reduced viability and proliferation, and decreased the migration and tube formation of HRVECs under basal condition (Figure S9A-D). cZNF609 overexpression aggravated oxidative stress or hypoxic stress-induced HUVEC apoptosis as shown by increased caspase 3 activity (Figure S9E-F).

cZNF609 regulates endothelial cell function by acting as a miRNA sponge

cZNF609 was mainly expressed in the cytoplasm. We speculated that cZNF609 might regulate gene expression by acting as a miRNA sponge. We used CircNet database and Circular RNA Interactome database to predict the miRNAs that potentially bind to cZNF609. miR-615-5p was predicted as a common miRNA that potentially binds to cZNF609 (Figure 4A, S10 and Table S1). miRNAs usually play their roles by binding to Ago2, the core part of RNA induced silencing complex (RISC). RNA immunoprecipitation (RIP) assays showed that cZNF609 was enriched in Ago2-containing immunoprecipitates compared with the control, immunoglobulin G (IgG) immunoprecipitates (Figure 4B). Moreover, miR-615-5p level in Ago2-containing immunoprecipitates was significantly higher than that in IgG immunoprecipitates (Figure 4B). We then inserted cZNF609 sequence into the downstream of luciferase reporter (LUC-cZNF609). miR-615-5p mimic transfection reduced the luciferase activity of LUC-cZNF609 to about 35%, but had no effect on the luciferase activity of LUC-cZNF609 mutant (Figure 4C). miR-615-5p mimic transfection had no effect on cZNF609 and ZNF609 mRNA expression (Figure 4D), suggesting that miR-615-5p did not affect cZNF609 and ZNF609 mRNA degradation. FISH assays showed that both cZNF609 and miR-615-5p was localized in the cytoplasm of HUVECs (Figure 4E). Using biotin-coupled miR-615-5p, we observed greater enrichment of cZNF609 in miR-615-5p-captured fraction compared to the negative control, biotinylated miR-335 (Figure 4F). We also observed greater enrichment of miR-615-5p in cZNF609-captured fraction compared to the negative control, biotinylated cZNF532 (Figure 4G). Moreover, we observed increased enrichment of cZNF609 in miR-615-5p-captured fraction compared to the negative control, biotinylated miR-335, upon high glucose and hypoxia stress (Figure 4H). These results suggest that cZNF609 serves as a binding platform for Ago2 and miR-615-5p, and may function as a miRNA sponge.

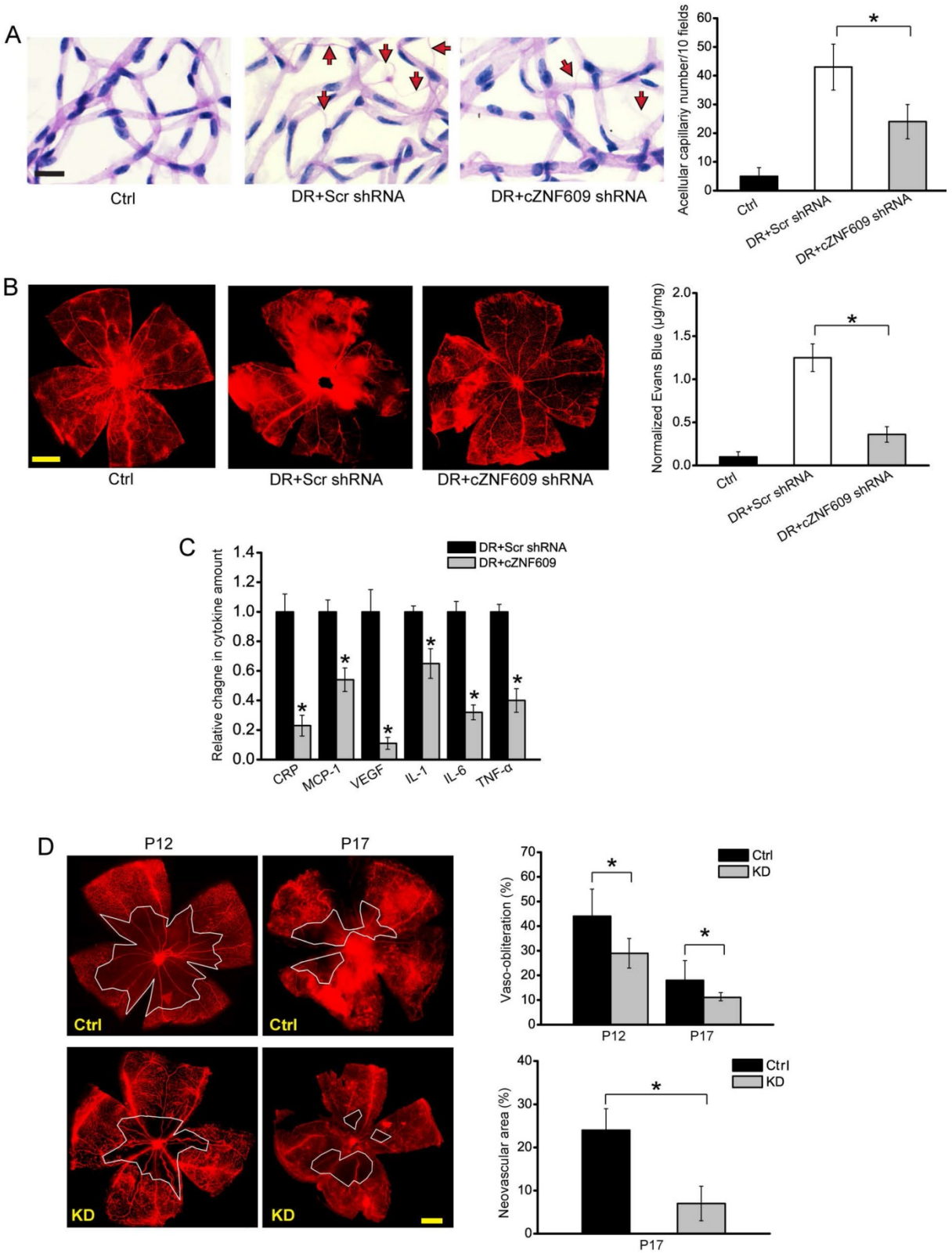

Figure 2. cZNF609 silencing decreases retinal vessel loss and suppresses pathological angiogenesis *in vivo* (A) Diabetic C57BL/6 mice (8-week old, male) were received an intravitreous injection of scrambled (Scr) shRNA, cZNF609 shRNA, or left untreated (Ctrl). Retinal trypsin digestion was performed to detect acellular capillaries. Acellular capillaries were quantified in 30 random fields per retina and averaged. Red arrows indicated acellular capillaries. Scale bar, 50 μm (n=5, *P<0.05). (B) The mice were infused with Evans blue dye for 2 h. Fluorescence images of flat-mounted retinas and quantification of Evans blue leakage was conducted. Scale bar, 500 μm (n=5, *P<0.05). (C) ELISA assays were conducted to detect the amount of C-reactive protein (CRP), MCP-1, VEGF, interleukin (IL)-1, IL-6, and TNF-α in retinal lysates (n=5, *P<0.05). (D) Retinal vaso-obliteration (VO) and neovascularization of cZNF609 silencing mice and matched control mice at P12 and P17 were shown by staining retinal vasculature using GS lectin-Alexa Flour 549. Avascular area was highlighted using white line. Scale bar: 100 μm. VO area (at P12 and P17) and pathologic angiogenic area (at P17) was statistically analyzed (n=5, *P<0.05). DR, diabetic retinopathy; Ctrl, control; KD, cZNF609 silencing. All data were from at least three independent experiments.

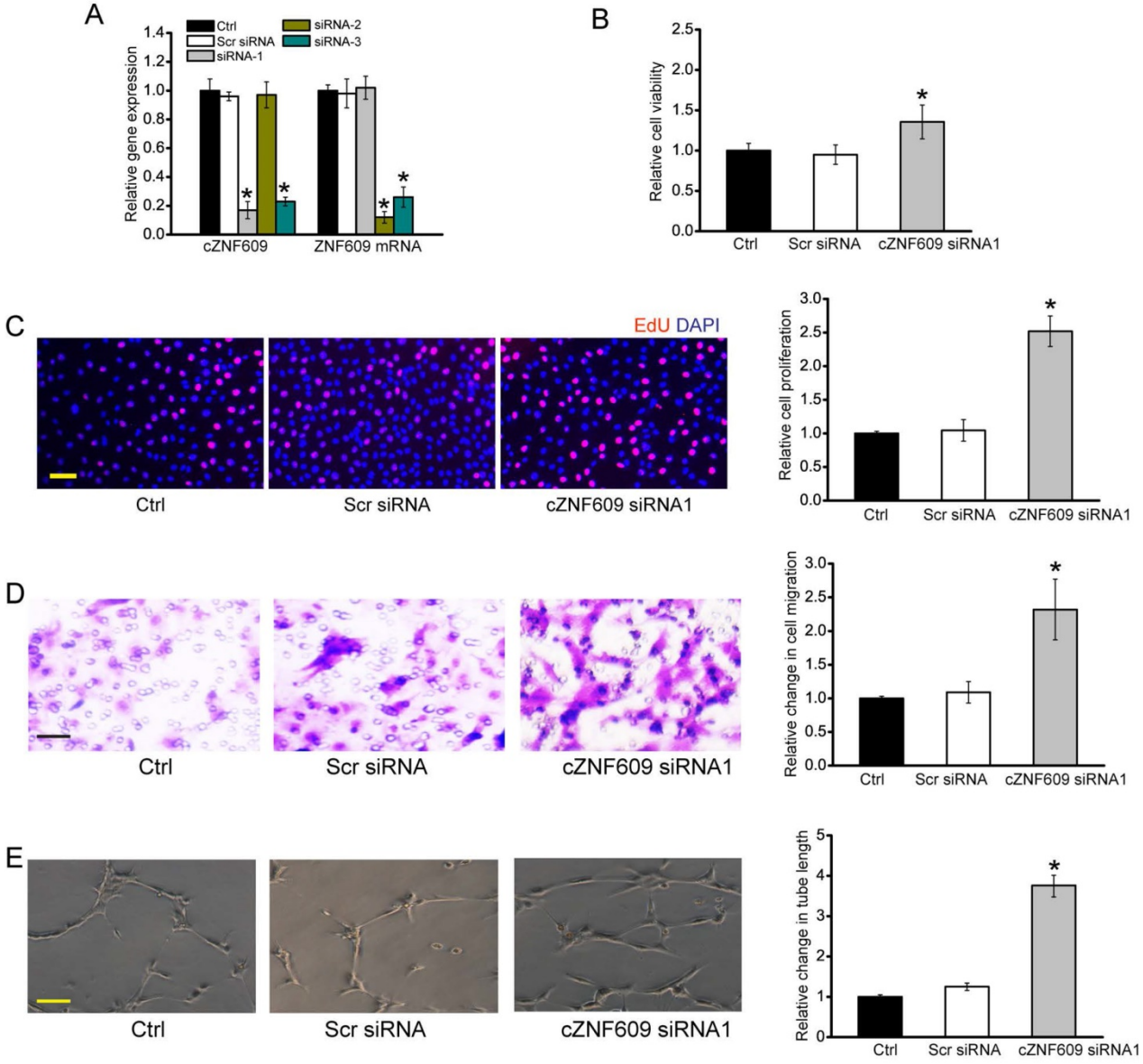

Figure 3. cZNF609 regulates endothelial cell function *in vitro* (A) HUVECs were transfected with scrambled siRNA (Scr), siRNA-1, siRNA-2, siRNA-3, or left untreated (Ctrl) for 48 h. qRT-PCRs were conducted to detect cZNF609 and ZNF609 mRNA expression (n=4, **P*<0.05). (B) Cell viability was detected using MTT method (n=4, **P*<0.05). (C) Cell proliferation was detected using EdU detection kit (Ribobio, Guangzhou, China) to analyze the incorporation of EdU during DNA synthesis (n=4, **P*<0.05). Scale bar, 200 μm. (D) Transwell assay and quantification analysis was conducted to detect HUVEC migration (n=4, **P*<0.05). Scale bar, 20 μm. (E) HUVECs were seeded on the matrigel matrix. The tube-like structures were observed 24 h after cell seeding. Average length of tube formation for each field was statistically analyzed (n= 4, **P*<0.05). Scale bar, 100 μm. All data were from at least three independent experiments.

miR-615-5p/cZNF609 interaction is involved in regulating endothelial cell function

Since miR-615-5p was sponged by cZNF609, we then determined the role of miR-615-5p *in vitro*. miR-615-5p mimic transfection partially rescued HUVECs from oxidative stress or hypoxic stress-induced cell apoptosis as shown by less PI-positive cells and decreased caspase 3 activity. miR-615-5p mimic plus cZNF609 siRNA transfection further decreased PI-positive cell number and caspase 3 activity (Figure 5A, S11, and S12). miR-615-5p mimic transfection increased the migration and tube formation ability of HUVECs. miR-615-5p mimic plus cZNF609 siRNA transfection further increased the migration and tube formation ability of HUVECs (Figure 5B and 5C). We further revealed that cZNF609 overexpression could rescue the effects of miR-615-5p mimic transfection on HUVEC function (Figure S13). We also showed that miR-615-5p inhibitor transfection significantly increased oxidative stress or hypoxic stress-induced HUVEC apoptosis as shown by increased caspase 3 activity. Moreover, miR-615-5p inhibitor transfection significantly reduced the migration and tube formation ability of HUVECs (Figure S14).

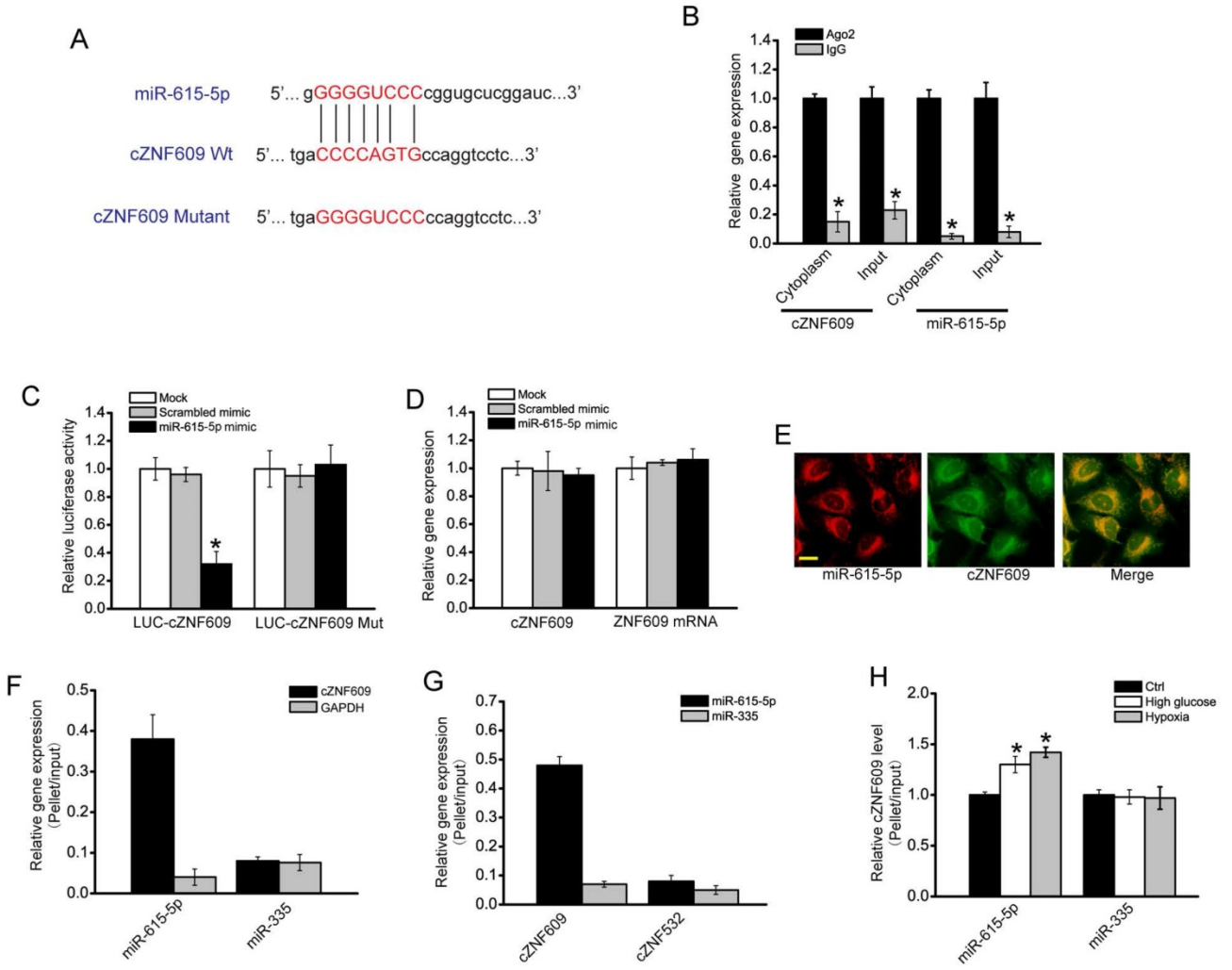

Figure 4. cZNF609 regulates endothelial cell function by acting as a miRNA sponge (A) Sequence alignment of wild-type miR-615-5p with cZNF609. Bottom: mutation in the cZNF609 sequence to generate the mutant luciferase reporter construct. (B) The cytoplasm and total cellular fractions were isolated from HUVECs, and immunoprecipitated using Ago2 or IgG antibody. cZNF609 and miR-615-5p amount in the immunoprecipitate was detected by qRT-PCRs (n=4, **P*<0.05). (C) HUVECs were co-transfected LUC-cZNF609 or LUC-cZNF609-mutant with miR-615-5p mimics or scrambled mimics. Luciferase activity was detected 48 h after transfection (n=4, **P*<0.05). (D) HUVECs were transfected with miR-615-5p mimics, scrambled mimics, or left untreated (Mock). qRT-PCRs were conducted to detect cZNF609 and ZNF609 mRNA expression. The data was shown as relative change compared with Mock group (n=4, **P*<0.05). (E) RNA-FISH assays were conducted to detect cZNF609 and miR-615-5p expression in HUVECs. miR-615-5p, red; cZNF609, green. Scale bar, 20 μm. (F) The 3'-end biotinylated miRNA duplexes were transfected into HUVECs. After streptavidin capture, cZNF609 and GAPDH mRNA levels in the input and bound fractions were determined by qRT-PCRs. The relative immunoprecipitate (IP)/input ratios were plotted. (G) The 3'-end biotinylated cZNF609 or cZNF532 was transfected into HUVECs. After streptavidin capture, miR-615-5p and miR-335 levels in the input and bound fractions were determined by qRT-PCRs. (H) The 3'-end biotinylated miRNA duplexes were transfected into HUVECs. These cells were then exposed to high glucose (30 mM) or $CoCl_2$ (200 μM), or left untreated for 48 h. After streptavidin capture, cZNF609 levels in the input and bound fractions were determined by qRT-PCRs. The relative immunoprecipitate (IP)/input ratios were plotted (n=4, **P*<0.05).

We also investigated whether the role of miR-615-5p in vascular dysfunction *in vivo*. In the model of diabetic retinopathy, miR-615-5p overexpression could mimic cZNF609 silencing on retinal vascular dysfunction. miR-615-5p overexpression could reduce diabetes mellitus-induced retinal vascular leakage (Figure 5D). miR-615-5p overexpression rescued hyperglycemia-induced aggravated capillary degeneration (Figure 5E). In the model of oxygen-induced retinopathy, miR-615-5p overexpression significantly decreased retinal vessel loss and suppressed pathological angiogenesis (Figure 5F).

cZNF609/miR-615-5p/MEF2A network is involved in regulating endothelial cell function

We then employed Targetscan database to predict the target genes of miR-615-5p. Three candidate genes including MEF2A, Tie2, and IGF2 were identified (Table S2), which are involved in angiogenesis and retinopathy [23]. In diabetic retinas, MEF2A, Tie2, and IGF2 expression was significantly up-regulated (Figure 6A). In the model of oxygen-induced retinopathy, MEF2A, Tie2, and IGF2 expression was significantly increased at the neovascularization stage (P12-P17) (Figure 6B).

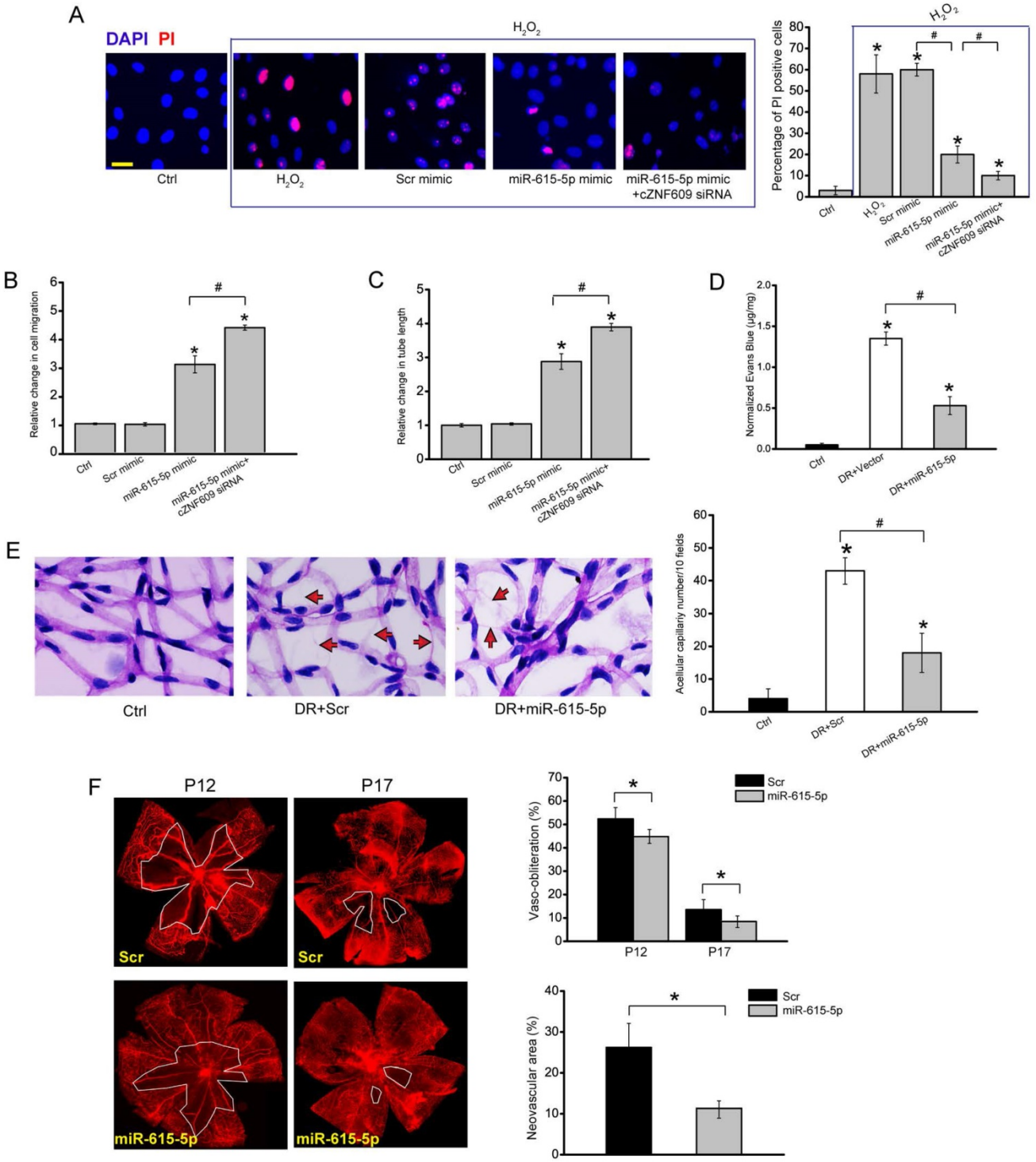

Figure 5. miR-615-5p/cZNF609 interaction is involved in regulating endothelial cell function (A) HUVECs were transfected with scrambled mimic (Scr), miR-615-5p mimic, miR-615-5p mimic plus cZNF609 siRNA, or left untreated, and then treated with or without H_2O_2 (100 μm) for 48 h. Apoptotic cells were analyzed using PI staining and quantified (n=4, **P*<0.05 versus Ctrl group). Scale bar: 20 μm. (B and C) HUVECs were transfected with miR-615-5p mimic, miR-615-5p mimic plus cZNF609 siRNA, or left untreated. Transwell assay and quantification analysis was conducted to detect endothelial cell migration (B, n=4, **P*<0.05 versus Ctrl group). The tube-like structures were observed 24 h after HUVEC seeding. Average length of tube formation for each field was statistically analyzed (C, n=4, **P*<0.05 versus Ctrl group). (D) Diabetic C57BL/6 mice (8-week old, male) were received an intravitreous injection of scrambled agomir (Scr), miR-615-5p agomir, or left untreated (Ctrl). These agomirs were injected once monthly for a total of 6 months. The mice were infused with Evans blue dye for 2 h. Fluorescence images of flat-mounted retinas and quantification of Evans blue leakage was conducted (n=5, **P*<0.05 versus Ctrl group). (E) Retinal trypsin digestion was conducted to detect acellular capillaries. Acellular capillaries were quantified in 30 random fields per retina and averaged. Red arrows indicated acellular capillaries. Scale bar, 50 μm (n=5, **P*<0.05 versus Ctrl group). (F) Retinal vaso-obliteration (VO) and neovascularization of miR-615 overexpression mice and matched control mice at P12 and P17 were shown by staining retinal vasculature using GS lectin-Alexa Flour 549. Avascular areas were highlighted using white lines. Scale bar: 100 μm. Quantification of VO area at P12 and P17 and angiogenic area at P17 was also conducted (n=5, **P*<0.05 versus Scr group). "#" indicated significant difference between the marked groups. All data were from at least three independent experiments.

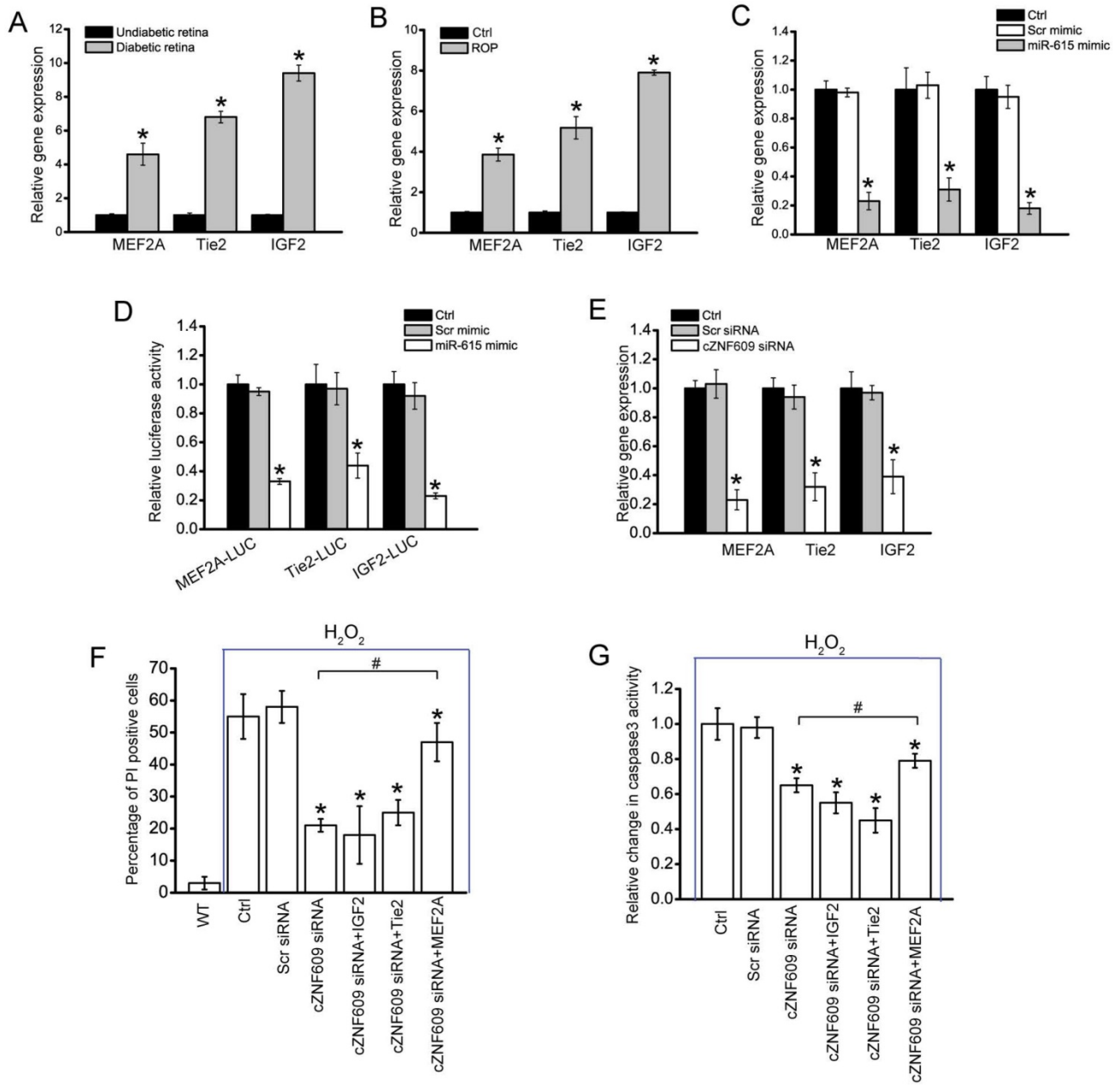

Figure 6. cZNF609/miR-615-5p/MEF2A network is involved in regulating endothelial cell function (A) qRT-PCRs were conducted to compare retinal MEF2A, Tie2, and IGF2 expression between 6-month diabetic C57BL/6 mice and age-matched un-diabetic C57BL/6 mice (n=6 animals per group). (B) Neonatal mice were exposed to 75% oxygen from P7 to P12, and then returned to room air. qRT-PCRs were conducted to compare retinal MEF2A, Tie2, and IGF2 expression between untreated (Ctrl) and OIR retinas at P17 (n=6 animals per group, **P*<0.05). (C) HUVECs were transfected with miR-615-5p mimic, Scr miRNA mimic, or left untreated (Ctrl) for 48 h. qRT-PCRs were conducted to detect MEF2A, Tie2, and IGF2 expression (n=4, **P*<0.05). (D) HUVECs were co-transfected LUC-MEF2A, LUC-Tie2, or LUC-IGF2 with miRNA mimic. Luciferase activity was detected using the dual luciferase assay 48 h after transfection (n=4, **P*<0.05). (E) HUVECs were transfected with Scr siRNA, cZNF609 siRNA, or left untreated (Ctrl) for 48 h. qRT-PCRs were conducted to detect MEF2A, Tie2, and IGF2 expression (n=4, **P*<0.05). (F and G) HUVECs were treated as shown for 48 h. Cell apoptosis was determined using PI staining and caspase 3 activity kit. "*" indicated significant difference compared with the group only treated with H_2O_2. "#" indicated significant difference between the marked groups (n=4).

miR-615-5p mimic transfection significantly inhibited MEF2A, Tie2, and IGF2 expression in HUVECs (Figure 6C). By contrast, the expression of other angiogenic factors, fibroblast growth factor 2 (FGF2), NOTCH1, CXCR4, low-density lipoprotein receptor-related protein 5 (LRP5), and LRP6, was not affected by miR-615-5p mimic transfection (Figure S15). Direct regulation of miR-615-5p on its angiogenic targets was further supported by luciferase reporter assays. miR-615-5p mimic transfection decreased the luciferasem activities of reporter constructs containing target sequences of MEF2A, Tie2, and IGF2 (Figure 6D). These results suggest that miR-615-5p is a direct regulator of

MEF2A, Tie2, and IGF2 in endothelial cells. We also showed that cZNF609 silencing significantly reduced MEF2A, Tie2, and IGF2 expression (Figure 6E). Further functional analysis revealed that cZNF609 silencing increased the migration and tube formation ability of HUVECs, and rescued HUVECs from oxidative stress or hypoxia-induced apoptosis. MEF2A but not Tie2 or IGF2 silencing could mimic the effect of cZNF609 silencing. Moreover, MEF2A but not Tie2 or IGF2 overexpression could rescue cZNF609 silencing-mediated effects on HUVEC migration, tube formation, and apoptosis (Figure 6F, 6G and S16). We thus concluded that MEF2A-cZNF609 crosstalk is involved in regulating endothelial cell function.

Clinical relevance of cZNF609 dysregulation in vascular diseases

To translate our findings to a physiologically relevant context, we determined the role of cZNF609 in primary human retinal endothelial cells. cZNF609 siRNA transfection significantly down-regulated cZNF609 expression (Figure 7A). cZNF609 silencing increased the viability, proliferation, migration, and tube formation of human retinal endothelial cells (Figure 7B-E).

We further determined cZNF609 and miR-615-5p expression pattern in clinical samples. cZNF609 expression in the fibrovascular membranes of diabetic patients was significantly higher than that in the idiopathic epiretinal membranes of non-diabetic patients (Figure 7F and Table S3). cZNF609 expression was up-regulated in the plasma fraction of peripheral blood of diabetic patients compared with non-diabetic controls (Figure 7G and Table S4). By contrast, miR-615-5p had an opposite expression pattern in fibrovascular membranes and peripheral blood of diabetic patients (Figure S17A and S17B).

Endothelial dysfunction and injury plays an important role in the pathogenesis of several cardiovascular diseases, such as coronary artery disease and hypertension [24]. We found that circulating levels of cZNF609 were down-regulated in the patients with coronary artery disease (CAD) or hypertension compared with healthy volunteers (Figure 7H, Table S5, Figure 7I, and Table S6). By contrast, circulating levels of miR-615-5p were significantly up-regulated in the patients with coronary artery disease (CAD) or hypertension (Figure S17C and S17D). Collectively, these results implicate that cZNF609 is involved in the pathogenesis of vascular dysfunction.

Discussion

In this study, we show that cZNF609 silencing decreases retinal vessel loss and pathological angiogenesis *in vivo*. cZNF609 also regulates endothelial cell function *in vitro*. Mechanistically, cZNF609 acts as an endogenous miR-615 sponge to sequester and inhibit miR-615 activity, which leads to increased MEF2A expression. This study provides novel insights for understanding the pathogenesis of vascular dysfunction.

The retina is a good model to investigate developmental and pathological angiogenesis [25]. cZNF609 is abundantly expressed in endothelial cells, and is dysregulated upon vascular dysfunction. We thus are interested in the potential role that cZNF609 could play in the retina in developmental and pathologic settings. Under normal condition, cZNF609 silencing increases endothelial cell viability and proliferation, and accelerates endothelial cell migration and tube formation *in vitro*, suggesting a pro-angiogenic role. However, cZNF609 silencing has no effect on normal retinal developmental angiogenesis. Retinal developmental angiogenesis is an intricate and complex process mediated by the coordinated response of vascular endothelial and mural cells to the angiogenic cues. The crosstalk between endothelial cell and other vascular-related cells is critical for maintaining vascular function [26]. Although cZNF609 silencing affects endothelial cell function *in vitro*, cZNF609 silencing-mediated endothelial cell dysfunction would be interrupted or reversed by the participation of other vascular-related cells *in vivo*. This reason could partially account for why cZNF609 silencing affects endothelial cell function in vitro but does not affect retinal developmental angiogenesis *in vivo*.

In DR model, hyperglycaemia could lead to increased oxidative stress for ECs and up-regulate cZNF609 expression. cZHF609 silencing could help retinal ECs to combat against oxidative stress and decrease vascular injury, in turn leading to decreased hypoxic area and pathological angiogenesis. In OIR animal model, mice undergo hyperoxia phase and subsequent phase of relative hypoxia that commence when mice are returned to a room air environment. cZHF609 silencing could help ECs to combat against hypoxia stress and decreases pathological angiogenesis. Direct inhibition of pathological angiogenesis or reducing retinal vessel loss could ameliorate retinopathy [20, 27]. We also complemented the studies in mice with in vitro studies in cultured HUVECs. cZNF609 silencing reduces oxidative stress or hypoxic stress-induced apoptosis in HUVECs. These in vitro findings are in line with the results in OIR and DR.

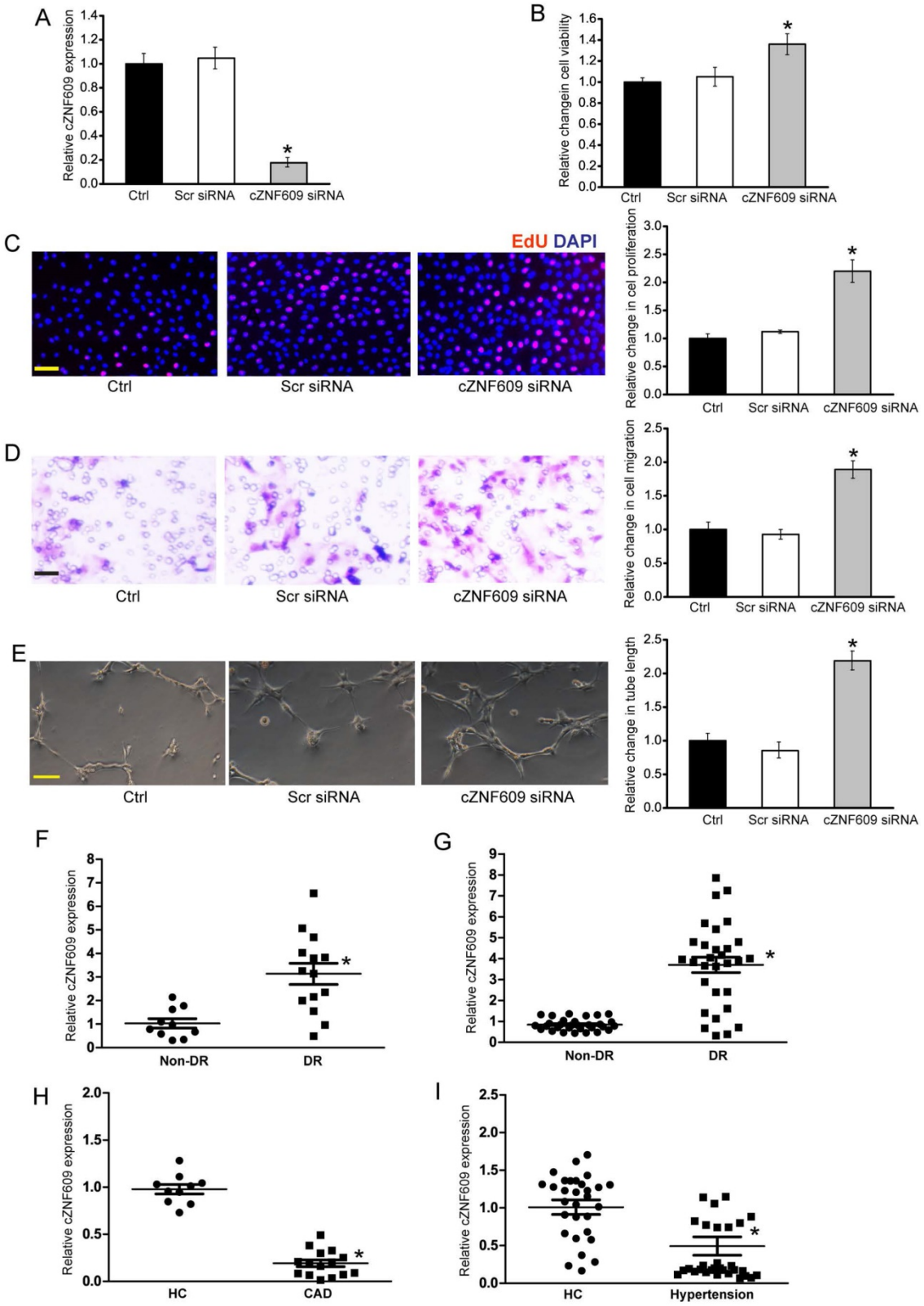

Figure 7. Clinical relevance of cZNF609 dysregulation in vascular disease (A) Human retinal endothelial cells were transfected with scrambled siRNA (Scr), cZNF609 siRNA, or left untreated (Ctrl) for 48 h. qRT-PCRs were conducted to detect cZNF609 expression (n=4, *P<0.05). (B) Cell viability was determined by MTT assay. Result was shown as relative change compared with Ctrl group (n=4, *P<0.05). (C) Cell proliferation was detected by EdU detection kit (n=4, *P<0.05). Scale bar, 200 μm. (D) Transwell assay and quantification analysis was used to detect cell migration (n=4, *P<0.05). Scale bar, 20 μm. (E) Human retinal endothelial cells were seeded on the matrigel matrix. Tube-like structures were observed 24 h after cell seeding. Average length of tube formation for each field was statistically analyzed (n=4, *P<0.05). Scale bar, 100 μm. (F) qRT-PCRs were performed to detect cZNF609 expression in the fibrovascular membranes of diabetic patients (n=15) and idiopathic epiretinal membranes of non-diabetic patients (n=10) (*P<0.05 versus non-diabetic controls). (G) qRT-PCRs were conducted to detect cZNF609 expression in EDTA-plasma obtained from diabetic patients (n=30) and non-diabetic controls (n=30) (*P<0.05 versus non-diabetic controls). (H) cZNF609 expression in EDTA-plasma obtained from the patients with CAD (n=15) and healthy volunteers (HC; n=10) was determined by qRT-PCRs. (I) cZNF609 expression in EDTA-plasma obtained from patients with hypertension (n=30) and healthy volunteers (HC; n=30) was determined by qRT-PCRs.

In vitro studies also reveal that cZNF609 silencing increases endothelial cell viability, proliferation, migration, and tube formation, suggesting a pro-angiogenic role. Retinal angiogenesis could lead to severe loss of vision due to increased vascular permeability, retinal edema, vascular fragility, or fibrovascular proliferation [28]. *In vivo* studies show that cZNF609 silencing decreases pathological angiogenesis, inflammatory reaction, and vascular permeability, which seemingly contradicts with the result of *in vitro* studies. In fact, cZHF609 silencing could help retinal ECs to combat against stress, decrease vascular injury, thereby reducing pathological angiogenesis. Ongoing clinical trials reveal that both pro- and antiangiogenic treatments with single angiogenic molecules is more challenging than anticipated. A single angiogenesis inhibitor may not suffice to combat against pathological angiogenesis [29]. As building new, functional and durable vessel requires the interplay of multiple signaling molecular, cZNF609-mediated regulatory networks would be involved in this process. Thus, it is important to maintain a relative balance of cZNF609 level *in vivo*. One the one hand, we could interfere cZNF609 expression to play its role against stresses. One the other hand, the coordination of the expression of cZNF609 and its interacting factors is critical for controlling pathological angiogenesis.

We also investigated the mechanism of angiogenic action of cZNF609. circRNAs may act as endogenous sponge RNAs to interact with miRNAs and affect the expression of miRNA target genes [30]. ciRS-7/CDR1as and Sry circRNA act as inhibitors of miRNA function by binding miRNAs [31, 32]. Circular RNA-HRCR acts as miR-223 sponge to regulate cardiac hypertrophy and heart failure [10]. We show that cZNF609 functions as an endogenous miR-615-5p sponge to sequester and inhibit miR-615-5p activity. A previous study has been reported that cZNF609 takes part in the onset of Hirschsprung disease (HSCR) through the crosstalk with AKT3 by competing for shared miR-150-5p [33]. Recently, whether circular RNAs play their roles by acting as ceRNA sponges remains controversial. Given the low expression of most circular RNAs, overexpression of competing endogenous RNAs may has little effect on miR bio-availability and function. A recent computational study also shows that of 7112 human circRNAs identified in the ENCODE data sets, only 2 circRNAs own more predicted miRNA binding sites than expected by chance; thus, arguing against the generalization of circRNAs as miRNA sponges [34]. We determine the relative expression abundance of cZNF609 and miR-615-5p in mouse retinas, and show that cZNF609 has similar expression abundance as miR-615-5p (Figure S18). Increased cZNF609 may sponge and sequester miR-615-5p upon high glucose or oxidative stress, releasing miR-615-5p-mediated repressive effects. cZNF609/miR-615-5p/target genes constitute a regulatory network. A slight change in cZNF609 level may alter miR-615-5p-mediated network. This network provides more precise gene regulation during vascular dysfunction.

Tie2, IGF2, and MEF2A were identified as the target genes of miR-615-5p. Tie2 is a tyrosine-protein kinase that regulates angiogenesis and endothelial cell function [35]. IGF2 regulates endothelial cell function by promoting migration, tube formation and production of vasodilator nitric oxide [36]. MEF2A activation is tightly associated with vascular endothelial cell function [37]. MEF2A but not Tie2 or IGF2 silencing could mimic the effects of cZNF609 silencing. MEF2A overexpression reverses cZNF609 silencing-mediated effects on cell migration, tube formation, and apoptosis. During vascular dysfunction, cZNF609 overexpression becomes a sink for miR-615-5p, and releases the repressive effect of miR-615-5p on MEF2A expression. cZNF609/miR-615-5p/MEF2A network is responsible for regulating vascular function.

It is becoming increasingly appreciated that reducing retinal avascularity and increasing revascularization has become important therapeutic strategies for ischemic retinopathies and cardiovascular diseases [38]. cZNF609 silencing protects retinal vasculature against degeneration, decreases retinal vessel loss, and suppresses pathological angiogenesis. The clinical relevance of cZNF609 is confirmed by the fact that circulating cZNF609 was dysregulated in some cardiovascular diseases. Circulating levels of cZNF609 were significantly down-regulated in the patients with CAD or hypertension compared with healthy volunteers. Hypertension or hyperlipidemia could lead to EC injury and apoptosis, generating a dysfunctional arterial endothelium. Endothelial integrity is usually maintained through the replacement of damaged ECs with proliferating and healthy ECs [39]. cZNF609 down-regulation in endothelial cells may be a compensatory response upon stress. cZNF609 silencing could protect endothelial cells against stress, and also contributes to the revascularization in ischemic diseases. Indeed, the role of cZNF609 in other cardiovascular diseases deserves further exploration.

This study provides clear evidence for a critical role of cZNF609 in mediating vascular dysfunction. We thus propose a candidacy of cZNF609 as a potential therapeutic target for treating vascular

diseases. cZNF609/miR-615-5p/MEF2A constitutes a network to protect endothelial cells against stress in vitro, and partially reverses retinal vessel loss, pathological angiogenesis, and inflammatory response in vivo. If we can develop a drug targeting cZNF609 or its interacting molecules, we may provide new therapeutic targets for treating vascular diseases. Previous studies have shown that targeting VEGF molecules is beneficial for treating retinal vascular dysfunction [40]. We speculate that co-targeting both cZNF609 and its interacting molecules may enhance the treatment efficacy of vascular diseases. Of course, these assumptions will require more experiments to validate and more clinical studies to verify.

Conclusions

In conclusion, this study demonstrates that cZNF609 is involved in vascular dysfunction. cZNF609 silencing decreases retinal vessel loss and suppresses pathological angiogenesis *in vivo*, and protects endothelial cell against oxidative stress and hypoxia stress *in vitro*. cZNF609 regulates vascular dysfunction through a signaling network which is composed of cZNF609, miR-615-5p, and MEF2A. These results help us to understand the mechanism of cZNF609-mediated vascular dysfunction, and might provide a therapeutic target for treating vascular diseases.

Acknowledgments

This work was generously supported by the grants from the National Natural Science Foundation of China (Grant No. 81470594 to B.Y., Grant No. 81371055 and 81570859 to Q.J., and Grant No. 81670878 to J.Y.), the grant from the Shanghai Youth Talent Support Program (to B.Y.), the grant from the Scientific Research Start-up Funding for Advanced Talents (to B.Y.), and the grant from the Young Scientists Program from Eye & ENT Hospital (to B.Y.).

Supplementary Material

Supplementary figures and tables.
http://www.thno.org/v07p2863s1.pdf

Competing Interests

The authors have declared that no competing interest exists.

References

1. Puro DG, Kohmoto R, Fujita Y, Gardner TW, Padovani-Claudio DA. Bioelectric impact of pathological angiogenesis on vascular function. *P Natl Acad Sci USA* 2016; 113(35):9934-9
2. Folkman J. Angiogenesis. *Annu Rev Med*. 2006; 57: 1-18
3. Carmeliet P. Angiogenesis in health and disease. *Nat Med*. 2003; 9: 653-60.
4. Sena CM, Pereira AM, Seiça R. Endothelial dysfunction—a major mediator of diabetic vascular disease. *Biochim Biophys Acta*. 2013; 1832: 2216-31
5. Eelen G, de Zeeuw P, Simons M, Carmeliet P. Endothelial cell metabolism in normal and diseased vasculature. *Circ Res*. 2015; 116: 1231-44
6. Boeckel J-N, Jaé N, Heumüller AW, Chen W, Boon RA, Stellos K, et al. Identification and characterization of hypoxia-regulated endothelial circular RNA. *Circ Res*. 2015; 117: 884-90
7. Salzman J. Circular RNA expression: its potential regulation and function. *Trends Genet*. 2016; 32: 309-16
8. Salzman J, Chen RE, Olsen MN, Wang PL, Brown PO. Cell-type specific features of circular RNA expression. *PLoS Genet*. 2013; 9: e1003777
9. Zheng Q, Bao C, Guo W, Li S, Chen J, Chen B, et al. Circular RNA profiling reveals an abundant circHIPK3 that regulates cell growth by sponging multiple miRNAs. *Nat Commun*. 2016; 7: 11215
10. Wang K, Long B, Liu F, Wang J-X, Liu C-Y, Zhao B, et al. A circular RNA protects the heart from pathological hypertrophy and heart failure by targeting miR-223. *Eur Heart J*. 2016; 37 (33): 2602-11
11. Holdt LM, Stahringer A, Sass K, Pichler G, Kulak NA, Wilfert W, et al. Circular non-coding RNA ANRIL modulates ribosomal RNA maturation and atherosclerosis in humans. *Nat Commun*. 2016; 7: 12429
12. Yan B, Yao J, Liu J-Y, Li X-M, Wang X-Q, Li Y-J, et al. LncRNA-MIAT regulates microvascular dysfunction by functioning as a competing endogenous RNA. *Circ Res*. 2015; 116: 1143-56
13. Michalik KM, You X, Manavski Y, Doddaballapur A, Zörnig M, Braun T, et al. Long noncoding RNA MALAT1 regulates endothelial cell function and vessel growth. *Circ Res*. 2014; 114: 1389-97
14. Lyu D, Huang S. The emerging role and clinical implication of human exonic circular RNA. *RNA Biol*. 2016: 1-7
15. Flammer J, Konieczka K, Bruno RM, Virdis A, Flammer AJ, Taddei S. The eye and the heart. *Eur Heart J*. 2013; 34: 1270-8
16. Glažar P, Papavasileiou P, Rajewsky N. circBase: a database for circular RNAs. *RNA*. 2014; 20: 1666-70
17. Rybak-Wolf A, Stottmeister C, Glažar P, Jens M, Pino N, Giusti S, et al. Circular RNAs in the mammalian brain are highly abundant, conserved, and dynamically expressed. *Mol Cell*. 2015; 58: 870-85
18. Laity JH, Lee BM, Wright PE. Zinc finger proteins: new insights into structural and functional diversity. *Curr Opin Struc Biol*. 2001; 11: 39-46
19. Smith L, Wesolowski E, McLellan A, Kostyk SK, D'Amato R, Sullivan R, et al. Oxygen-induced retinopathy in the mouse. *Invest Ophth Vis Sci*. 1994; 35: 101-11
20. Xu Z, Gong J, Maiti D, Vong L, Wu L, Schwarz JJ, et al. MEF2C ablation in endothelial cells reduces retinal vessel loss and suppresses pathologic retinal neovascularization in oxygen-induced retinopathy. *Am J Pathol*. 2012; 180: 2548-60
21. Behrendt D, Ganz P. Endothelial function: from vascular biology to clinical applications. *Am J Cardiol*. 2002; 90: L40-8
22. Giacco F, Brownlee M. Oxidative stress and diabetic complications. *Circ Res*. 2010; 107: 1058-70
23. Qazi Y, Maddula S, Ambati BK. Mediators of ocular angiogenesis. *J Genet*. 2009; 88: 495-515
24. Cai H, Harrison DG. Endothelial dysfunction in cardiovascular diseases: the role of oxidant stress. *Circ Res*. 2000; 87: 840-4
25. Stahl A, Connor KM, Sapieha P, Chen J, Dennison RJ, Krah NM, et al. The mouse retina as an angiogenesis model. *Invest Ophth Vis Sci*. 2010; 51: 2813-26
26. Chung AS, Ferrara N. Developmental and pathological angiogenesis. *Annu Rev Cell Dev Biol*. 2011; 27: 563-84
27. Sapieha P, Joyal J-S, Rivera JC, Kermorvant-Duchemin E, Sennlaub F, Hardy P, et al. Retinopathy of prematurity: understanding ischemic retinal vasculopathies at an extreme of life. *J Clin Invest* 2010; 120: 3022-32
28. Gariano RF, Gardner TW. Retinal angiogenesis in development and disease. *Nature*. 2004; 438: 960-6
29. Jain RK. Normalization of tumor vasculature: an emerging concept in antiangiogenic therapy. *Science*. 2005; 307: 58-62
30. Chen L-L. The biogenesis and emerging roles of circular RNAs. *Nat Rev Mol Cell Bio*. 2016;17(4):205-11
31. Hansen TB, Jensen TI, Clausen BH, Bramsen JB, Finsen B, Damgaard CK, et al. Natural RNA circles function as efficient microRNA sponges. *Nature*. 2013; 495: 384-8
32. Memczak S, Jens M, Elefsinioti A, Torti F, Krueger J, Rybak A, et al. Circular RNAs are a large class of animal RNAs with regulatory potency. *Nature*. 2013; 495: 333-8
33. Peng L, Chen G, Zhu Z, Shen Z, Du C, Zang R, et al. Circular RNA ZNF609 functions as a competitive endogenous RNA to regulate AKT3 expression by sponging miR-150-5p in Hirschsprung's disease. *Oncotarget*. 2016; 8: 808-18
34. Militello G, Weirick T, John D, Döring C, Dimmeler S, Uchida S. Screening and validation of lncRNAs and circRNAs as miRNA sponges. *Brief Bioinform*. 2016;: bbw053
35. Jones N, Dumont DJ. Tek/Tie2 signaling: new and old partners. *Cancer Metast Rev*. 2000; 19: 13-7
36. Bach LA. Endothelial cells and the IGF system. *J Mol Endocrinol*. 2015; 54: R1-R13
37. Hamik A, Wang B, Jain MK. Transcriptional regulators of angiogenesis. *Arterioscler Thromb Vasc Biol*. 2006; 26: 1936-47
38. McCarty MF, Liu W, Fan F, Parikh A, Reimuth N, Stoeltzing O, et al. Promises and pitfalls of anti-angiogenic therapy in clinical trials. *Trends Mol Med*. 2003; 9: 53-8
39. Shan K, Jiang Q, Wang X-Q, Yang H, Yao M-D, Liu C, et al. Role of long non-coding RNA-RNCR3 in atherosclerosis-related vascular dysfunction. *Cell Death Dis*. 2016; 7: e2248

40. Brownlee M. Biochemistry and molecular cell biology of diabetic complications. *Nature*. 2001; 414: 813-20